ISSN 2347-3487
Volume 11, Number 9
Journal of Advances in Physics

Structural and Physical Properties Study of Some Phosphate Glasses Used for Radiation Shielding

T. Z. Amer
Phys. Dept., Faculty of Science (Girls Branch), Al-Azhar Univ., Cairo, Egypt.
htagma@hotmail.com

ABSTRACT

Mossbauer Effect (ME) and Infrared (IR) spectroscopes are used to study the structure of some iron-sodium phosphate glasses containing strontium, with composition [(70-x) mol% P_2O_5. x mol% SrO, 15 mol% Fe_2O_3.15 mol% Na_2O, where x= 3, 6,9,12 and 15]. These glasses can have many interesting applications especially as gamma ray attenuators.

The amorphous nature and the glassy state character of these glasses can be confirmed from comparing the experimental and empirical values of both their density and molar volume. It was found that, as SrO was gradually increased the density increased while the molar volume decreased which may be due to the gradual decrease of the number of oxygen ion density in the glass networks.

The micro-hardness and magnetic susceptibility are also increased, which can be attributed to the gradual migration of iron from glass network modifier (GNM) to glass network former (GNF) positions, as confirmed by IR and ME results. IR and ME analysis indicated that both ferric and ferrous have tetrahedral and octahedral symmetry respectively and acting as GNF and GNM at different SrO contents. The gradual replacement of P_2O_5 by SrO force the iron to transfer from GNM to GNF.

The gamma-ray mass attenuation coefficient increased with the gradual increase of Sr^{2+} as heavy metal, while the HVL decreased. On the other hand the attenuation coefficient decreased with the increase of gamma-ray photon energy. So, these glasses can be used as transparent shielding materials for low gamma-ray energies and to capsulate the radio-active wastes, while the sample containing 15 mol% SrO, exhibits the highest attenuation coefficient.

KEYWORDS

Phosphate glass – radiation shielding - Mossbauer spectroscopy – FTIR analysis - density - molar volume

INTRODUCTION

During the last few decades, the use of radio-active sources is widely spread in various fields of our daily life. So, it is of interest to search for suitable shielding materials that can be used to protect mankind from hazard radiation, specially the contact users. Accordingly, many articles have been published aiming to investigate various types of glasses for such problem [1-3]. This is because, glasses are considered to be preferable shielding materials than those classically used, since glasses can be easily manufactured and shaped, in addition to their ability to transmit visible light and deprived toxicity [4].

Among all the well-known glass types, phosphates appeared to be of special interest, in spite of their hygroscopic nature, since the addition of 30 mol% metallic cations improves well their aqueous durability and hardness [5]. However, iron-sodium phosphate glasses are widely used due to their high aqueous durability and high hardness level, in addition to their potential applications. These glasses found now many interesting applications, where they can be used as semi-conductors [6], gamma-ray attenuators [7] and to vitrify high level radio-active wastes in addition to their usage as smart windows [8].

However, in this article some iron-sodium-phosphate glasses containing varying amounts of strontium oxide (as a heavy metal) have been prepared and were thoroughly investigated from the structural and physical properties points of view. Special interest was subjected to their gamma-ray attenuation properties as well as their ability to capsulate radio-active wastes.

EXPERIMENTAL WORK

Ammonium di-hydrogen phosphate, sodium carbonate, ferric oxide and strontium oxide were used as starting materials. The batches were weighted using an electric balance with four dismal digits and the desired weights were selected to give glasses obeying the following formula, [(70-x) mol% P_2O_5. x mol% SrO. 15 mol% Fe_2O_3. 15 mol% Na_2O], [Where, x = 3, 6, 9, 12 and 15]

The batches were melted in porcelain crucibles in an electric furnace, starting from RT and exacted at 250 ^oC for 2 h to expel the evaporated gasses, then the furnace was raised to 1100 ^oC and left for 2 h. The melts were stirred several times during melting to ensure complete mixing, and after the duration time, they quenched in air. The obtained glass samples, after just sitting were transferred directly to the annealing furnace at 250 ^oC for 2 h, to remove the internal stress then the furnace was turned off and was left to cool to RT.

The experimental density (ρ_{exp}) values were measured at room temperature using the liquid displacement method, applying Archimedes equation (1),

$$\rho_{exp} = \frac{M_a}{M_a - M_l}\rho_i \quad \text{..... (1)}$$

Where, M_a and M_l are the sample weights in air and liquid respectively.

ρ_l is the density of the used emersion liquid (carbon tetrachloride (CCl_4) ρ_l = 1.593 g/cm^3).

The empirical density values (ρ_{emp}) were also calculated applying equation (2),

$$\left(\rho_{emp}\right) = \sum x_i \rho_i \quad \text{..... (2)}$$

Where, ρ_i represents the densities of the oxides forming a glass sample.

X_i represents the mole fraction of corresponding oxide.

The molar volume $(V_m)_{exp}$ values were calculated using formula (3),

$$(V_m)_{exp} = \sum W_m \frac{1}{\rho_{exp}} \quad \text{..... (3)}$$

Where, W_m is the mean molecular weight of a glass sample,

ρ_{exp} is its experimental density.

Also, the empirical molar volume values $(V_m)_{emp}$ can be calculated when replacing (ρ_{exp}) by (ρ_{emp}) in equation (3), [9].

IR spectra of the studied glass samples were obtained in the wave number range (400-1400 cm^{-1}) using a computerized FTIR spectrometer model [NICOLET, FTIR-200], using KBr disk technique.

ME spectra were obtained at RT in a transmission geometry employing 10 mCi, ^{57}Co (in rhodium matrix) radioactive source and the obtained parameters were expressed relative to a metallic iron calibration spectrum. Two mathematical techniques were used to analyze the ME spectra of the studied samples,

1-The direct line shape technique based on Voigte profile was used to get the Mossbauer parameters (isomer shifts (IS), quadruple splitting (QS), line widths (LW) and the area of the different iron phases (Ar).

2- The distribution technique based on Lorentzian line shape was used to study the disordered in the glass samples.

Vicker's micro-hardness tester (Shimadzu HMv micro-hardness tester) for 10 sec with 20 g load was used to perform the micro-hardness measurements. The hardness values were calculated applying equation (4),

$$H_v = A\,(P/d^2) \qquad kg/mm^2 \quad \text{.....(4)}$$

Where, A is a constant equals 1854.4, P is the indentation load applied, and d is the mean value of the indentation diagonal [10].

The magnetic susceptibility of the studied glasses was also measured at RT using three Tesla electromagnets and four decimal digits electric balance.

The gamma-ray mass attenuation coefficients of the studied glasses have been also calculated using WIN-X-COM program based on the mixture rule [11], (equation (5)),

$$\left(\frac{\mu}{\rho}\right)_{m(total)} = \sum_{i=0}^{n} w_i \left(\frac{\mu}{\rho}\right)_{m(i)} \quad \text{..... (5)}$$

Where $(\mu/\rho)_m$ is the total mass attenuation coefficient for a glass sample and w_i is the fractional weight of each oxide in a glass sample.

The half value layers (HVL) of the studied glass were also calculated according to equation (6) [11]

$$HVL = \frac{0.693}{\mu} \quad \text{..... (6)}$$

where μ is the linear attenuation coefficient.

RESULTS AND DISCUSSION

Density and Molar Volume

Density of glass is a property of interest, since it reflects directly any structural changes or any crystalline phase formation. Fig. (1) Shows the variation of both the experimental and empirical density values with the increased of SrO content. It appeared that the empirical values increased linearly from 2.86 to 3.51 g/cm^3, while those of the experimental increased approximately in two different straight lines with different slopes, intersected at about 11 mol% SrO. Also, the empirical densities are usually higher than those of the experimental values.

On the other hand, the investigation of the molar volume of a glass is preferable than density, since it deals directly with the spatial structure of such glass.

Fig. (2) represents the variation of the experimental and empirical molar volume as SrO content was increased gradually, where both $(Vm)_{emp}$ and $(V_m)_{exp}$ values exhibit decreasing trends, The empirical molar volume ($(V_m)_{emp}$) decreased linearly from 45.6 to 40.3 cm^3/g.mole, while the experimental one ($(V_m)_{exp}$) decreased in two different straight lines with different slops, intersected at about 11 mol% SrO. Also, the values of $(V_m)_{emp}$ are usually of lower values than the corresponding $(V_m)_{exp}$ values which can be taken as evidences to confirm the amorphous nature and the glassy state character of the prepared glass samples [9].

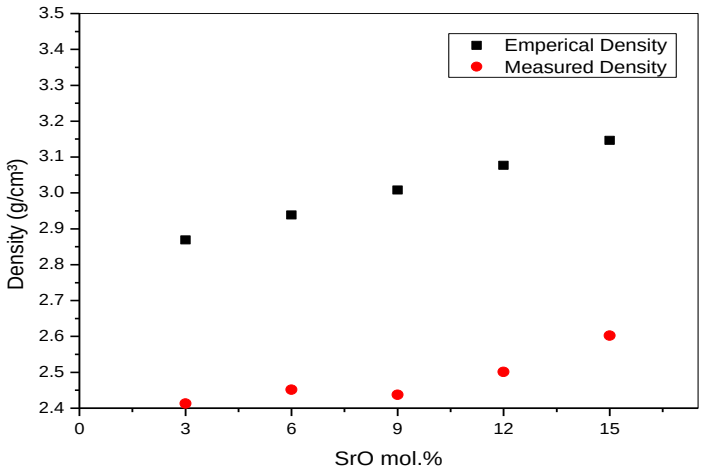

Fig.1: The variation of both the experimental and empirical densities versus SrO content.

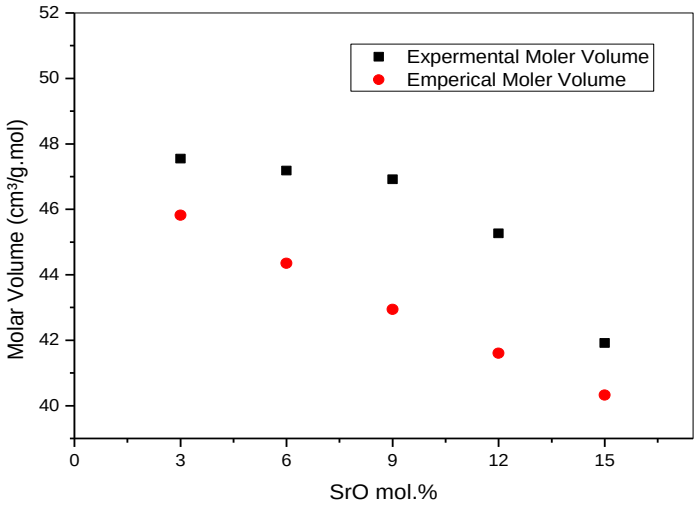

Fig.2: The variation of both the experimental and empirical molar volume values versus SrO content.

There are many factors affect directly the density and molar volume values, such as the difference in the density of both P_2O_5 and SrO [2.39 g/cm^3 & 4.70 g/cm^3 respectively], the differences in their molecular weights [141.935 & 103.819 respectively] , the differences in the atomic radii of the replaced cations [P (1.23 ^oA) & Sr (2.45 ^oA)] [19] and the variation in the number of oxygen ion density in the glass networks. Also, it can be supposed that some structural changes may take place.

Inspecting the above factors, it can be stated that a high density molecule SrO replaces a low density one (P_2O_5), but (P_2O_5) is of higher molecular weight than (SrO). However, it can be supposed that these two factors may act to counterbalance each other. It is known also that the atomic radius of Sr is approximately twice that of P, but since two P cations are replaced by a single Sr one, therefore this factor is also of little effect. However, it is of interest to investigate the effect of replacing P_2O_5 by SrO gradually on the number of oxygen ion density in the glass networks. The number of oxygen ion density can be now calculated applying the following equation (7) [13],

$$(N)_{O\text{-ion density}} = d\,[3(Wt/MW)_{Fe2O3} + (Wt/MW)_{Na2O} + 5(Wt/MW)_{P2O5}\ (Wt/MW)_{SrO}]\ N_A \text{ ------ (7)}$$

Where, d is the density of a sample, Wt is the mole fraction of an oxide, MW is the molecular weight of such oxide and N_A is Avogadro number.

Fig. (3), exhibits the variation of the $(N)_{O\text{-ion density}}$ as a function of SrO content, which shows approximately gradual linear decrease.

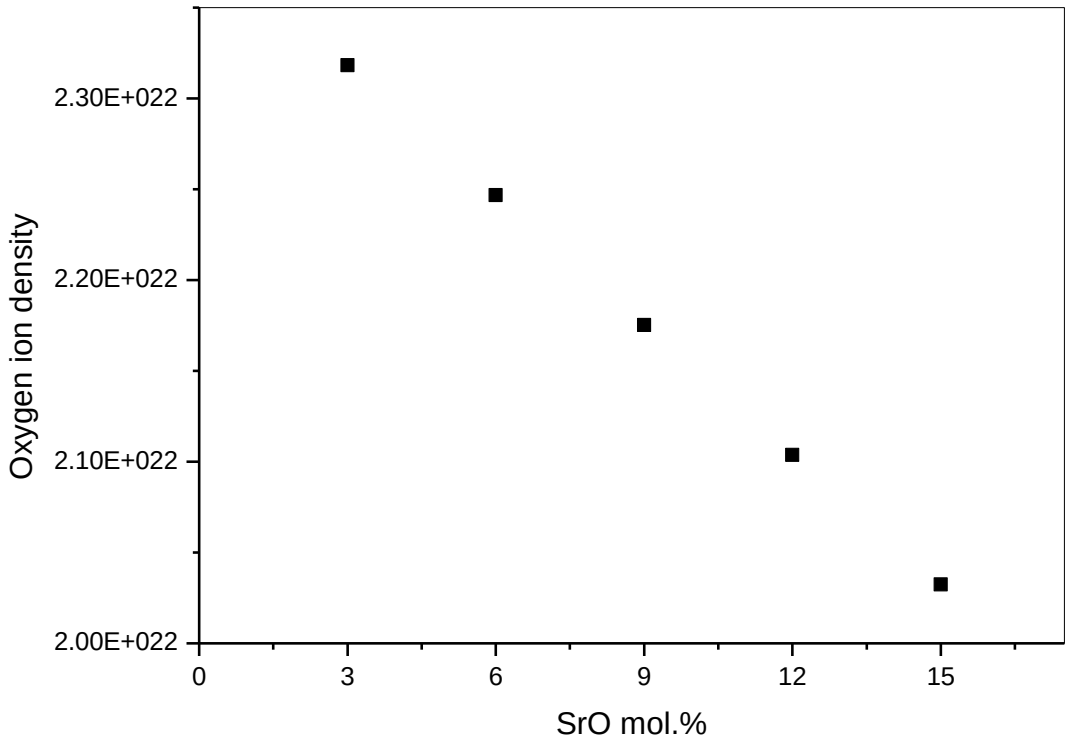

Fig.3: The variation of the number of oxygen ion density as a function of SrO content.

The gradual decrease of the molar volume can be now explained on the bases of the decrease in the number of oxygen ion density in the glass network. While, this decrease of volume with unchanging the samples weight can explain the gradual increase of the density.

The gradual decrease of the oxygen network continued with the gradual decrease of phosphorous as GNF cations forces the iron cations which occupy the GNM positions to migrate to the GNF positions. It is supposed also that, when P_2O_5 reaches only 59 mol%, the P == O may be untied to form $[PO_4]^-$, in addition to the increase in the number of the non-bridging oxygen in the glass network [5]. These two factors act to increase the ionic character of the glass network. However, this increase of the ionic character may be the reason of the observed change in the slope of both density and molar volume at about 11 mol% SrO.

FTIR Analysis

Fig. (4) Shows the obtained IR spectra of the samples containing 3 and 15 mol% SrO. The obtained data showed that there is a band at about 465 cm^{-1} which can be assigned to the bending vibration of O–P–O units [14]. The band that appeared at 490 cm^{-1}, can be attributed to the vibration of FeO_6 groups (Fe in octahedral site) in the glass network [15]. The intensities of this bands show a gradual decrease as SrO content was gradually increased which may be due to indicated that FeO_6 groups decreased gradually. The band appeared at about517 cm^{-1} can be attributed to O=P–O bending vibration [16]. Another band appeared at 550 cm^{-1}, can be assigned to the vibration of PO_4 groups (P in tetrahedral site) [16]. While the band appeared around 580 cm^{-1}, can be assigned to the vibration of the present FeO_4 units (Fe in tetrahedral site) in the glass networks, where its intensity shows gradual increase with the increase of SrO [7] indicating that FeO_4 content increased gradually also which may be due to that the Sr ions induced the iron ions to be in the four fold coordination.

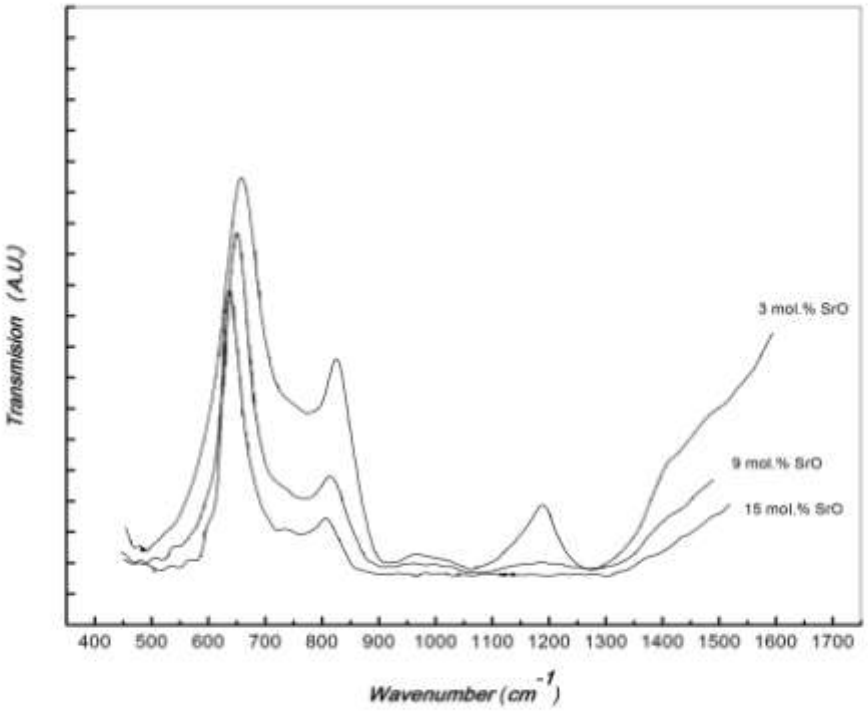

Fig.4: IR Spectra of the samples containing 3 and 15 mol% SrO as representative curve.

Other band appeared in the spectrum of the sample containing 3 mol% SrO, at 725 cm^{-1} can be attributed to symmetric stretching vibration of P—O—P bonds in Q^1 speech [18]. The band that appeared at about 815 cm^{-1}, can be attributed to the symmetric stretching vibration of P–O–P in phosphate rings [5]. At 920 cm^{-1}, there appeared a band which may be due to asymmetric stretching vibration of P—O—P bonds [19]. Two bands appeared around 1030 and 1110 cm^{-1}, these bands can be assigned to the vibration of $[PO4]^{3-}$ groups and $[P—O]^-$ bond vibration [18]. The band that appeared around 1250 cm^{-1} can be assigned to be due to $[PO_2]^-$, that is two non-bridging oxygen [16]. The band appeared at about 1290 may be due to the vibration of [P=O], and this band show a gradual decrease in its intensity with the gradual increase of SrO content until the complete vanishing in the spectrum of the sample containing 15 mol% SrO [20]. There appeared also a broad band in between 1300 and 1350 cm^{-1} which may be due to the appearance of some non-bridging oxygen anions [21]. Above 1400 cm^{-1} the bands appeared may be due to the vibrations of the present water groups which may be due to the used KBr technique [22].

The shifting of some bands may be due to some changes in the P-O-P bond angles and bond length which in turn due the high field strength of both Na^+ and Fe^{3+} cations and SrO. In addition, the gradual increase of the metallic cations act to shorten the length of phosphate chain in the network due to the depolymerization of phosphates and the increase of ionisity. It can be supposed also that some iron cations occupy the GNF positions and some others occupy the GNM positions, but with the gradual replacement of P_2O_5 By SrO, the iron in the NNM positions decreased while the iron in the GNF positions increased [5, 14].

Mossbauer spectroscopy

ME (gamma-ray resonance fluorescence) spectroscopy was early established to be an effective tool to study the hyperfine structure of iron cations in crystalline and amorphous solids. Fig. (5) represent the obtained Mossbauer spectra of the studied glass samples at room temperature (RT). The computer analysis and fitting show that all spectra (except that of the sample containing 15 mol% SrO) are composed of two different paramagnetic quadrupole doublets indicated that iron occupy two different states, nominated Fe(I) and Fe(II). The obtained hyperfine parameters are listed in Table (1), where the ME parameters of Fe(I) phase indicated that the iron cations appeared in ferric state occupying the tetrahedral coordination symmetry, while those of Fe(II) phase indicated that iron cations appeared in ferrous state occupying the octahedral coordination symmetry [23]. The appearance of some iron cations in the ferrous state, in spite of the addition of iron in the form of alpha-ferric oxide (Fe_2O_3) may be due to the reduction effect of phosphorus, which introduced as ammonium di-hydrogn phosphate ($NH_4H_2PO_4$). The appeared broadening in the doublet of the sample containing 15 mol% SrO, may be due to the formation of the non-bridging oxygen anions as indicated by the IR results.

ISSN 2347-3487
Volume 11, Number 9
Journal of Advances in Physics

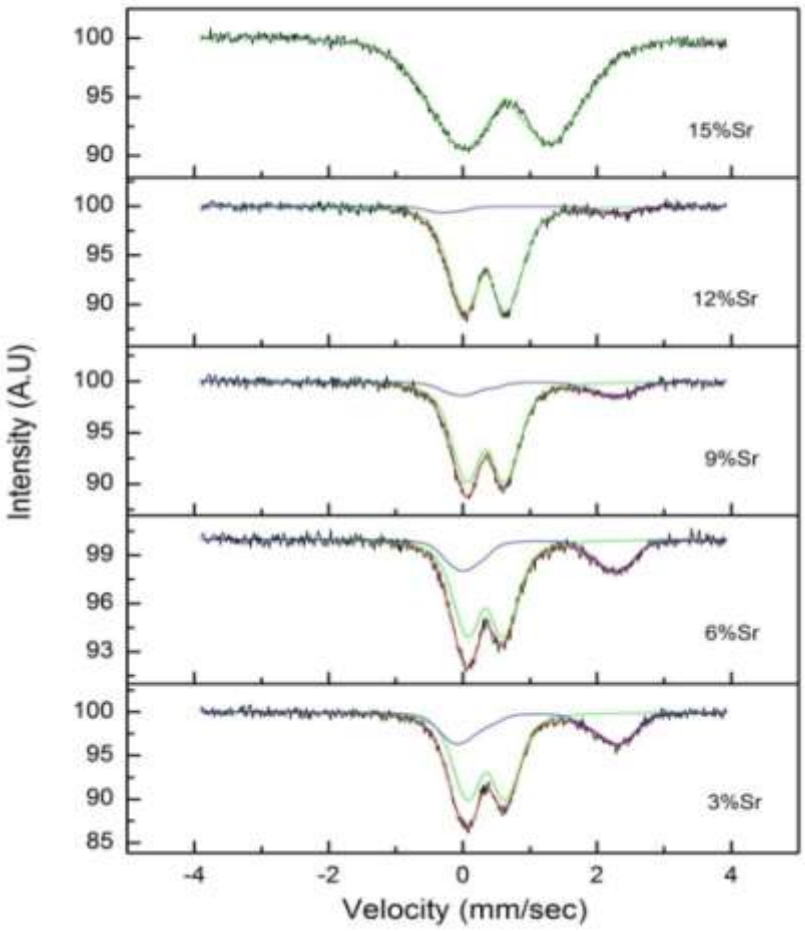

Fig.5: The obtained Mossbauer spectra for the studied glasses.

Table 1. The calculated Mossbauer parameters of the studied glass samples and their assignment.

	Fe^{3+}			assignment	Fe^{2+}			assignment
SrO%	**I.S (mm/sec)**	**Q.S (mm/sec)**	**Ar**		**I.S (mm/sec)**	**Q.S (mm/sec)**	**Ar**	
3	0.35	0.55	0.65	tetrahedral	1.114	2.422	0.347	octahedral
6	0.34	0.52	0.69	tetrahedral	1.14	2.291	0.31	octahedral
9	0.34	0.55	0.82	tetrahedral	1.126	2.227	0.175	octahedral
12	0.34	0.60	0.93	tetrahedral	1.025	2.75	0.0726	octahedral
15	0.69	1.27	1	tetrahedral	-	-	0	

Inspecting the obtained results in Table (1), and considering the area under the ME absorption peaks of both Fe^{2+} and Fe^{3+} states, it can be observed that, Fe^{3+} state increased while Fe^{2+} state decrease gradually. The variation of the ratio (Fe^{2+} /∑Fe) as a function of SrO content is exhibited in Fig. (6). The gradual decrease of such ratio continued with the gradual increase of SrO to reach zero at 15 mol% SrO. The appearance of some iron cations in the ferrous state, in spite of the addition of iron in the form of alpha-ferric oxide (Fe_2O_3) may be due to the reduction effect of phosphorous, which introduced as ammonium di-hydrogen phosphate ($NH_4H_2PO_4$). It is well known that this ratio affect approximately all the glass properties, and it depends on the glass composition and the preparation technique, due to the variation of the (O/P) and (Fe/P) molar ratios [24].

From another point of view and considering the coordination state of iron cations in the studied glasses, it is appeared that, in the sample containing only 3 mol% SrO, about 65% of the iron ions occupy the tetrahedral positions acting as GNF cations, while about 35% only occupy the octahedral positions acting as GNM, in the sample containing only 3 mol% SrO.

On going to higher SrO content glass, the relative amount of iron occupying GNF increased at the expense of iron in the GNM positions. This may be due to the gradual decrease of P_2O_5, and this was found in agreement with the IR results.

The quadrupole splitting distribution profiles of Fe^{3+} for all samples are illustrated in Fig. (7). It is seen that, the QS varied from 0 to 2 mm/s as SrO content increased up to 12 mol%, while it varied from 0 to 4 mm/s in the sample containing 15% SrO, as indicated in Table(1).

A remarkable smooth increase in the width of the distribution profile is observed with increasing SrO content which can be attributed to the gradual increase of the disorder in the glass network. The observed dramatic increase in the profile width of the sample containing 15% SrO confirms the high disordered of such network. This network is characterized by the presence of two different GNFs (phosphorous & iron) as well as two different GNMs (sodium & strontium, that is, an alkali and alkaline earth cations). Since the hyperfine parameters almost reflect the variation of the local distortion around iron in the network. However, the observed broadened quadrupole splitting in such sample may be due to the following factors:

1- Such sample undergoes various distributions of oxygen around iron in the glass network.
2- It undergoes an alkali-alkaline earth effect [25].
3- This sample contains the highest value of the NBOs anions [26].

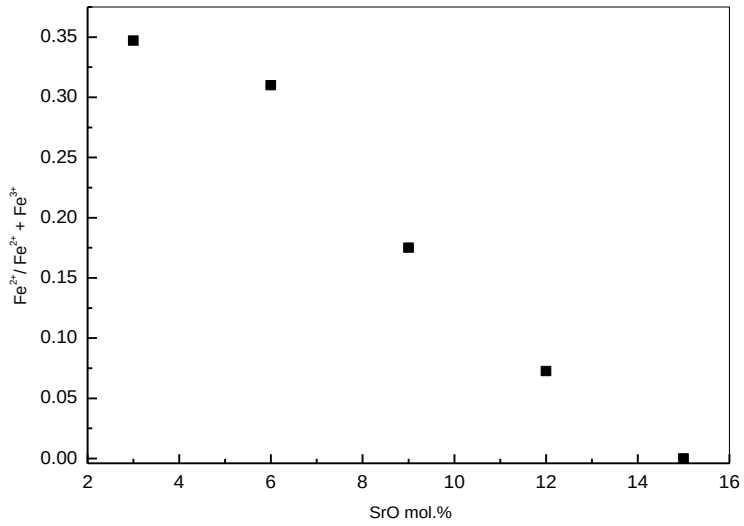

Fig.6: The variation of (Fe^{2+} /∑Fe) ratio as a function of SrO content.

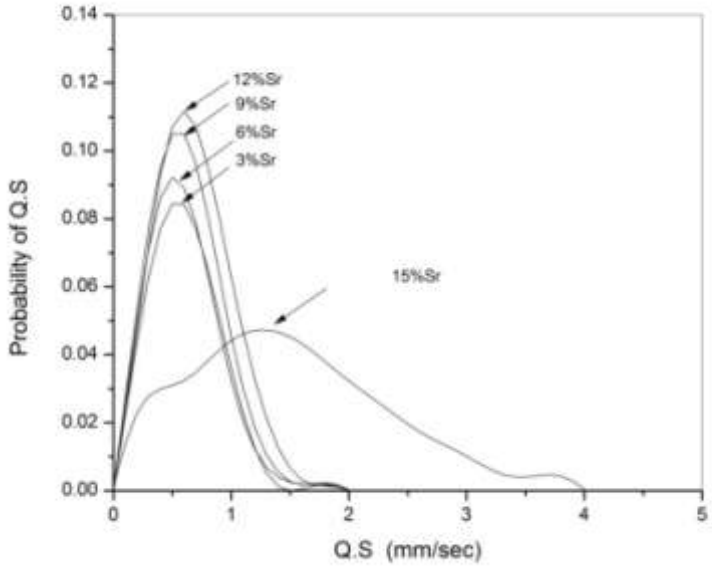

Fig.7: Quadrupole splitting distribution profiles for the studied glass samples.

The Mechanical Hardness

The hardness measurements were performed to characterize the behavior of the glass with permanent changes in the surface, glass strength, brittle fracture, crack growth and fatigue. The obtained hardness results show gradual increases from 314 to 398 kg/mm^2 with increasing SrO at the expense of P_2O_5 contents. This can be attributed to the introduced strontium as heavy metal cations, and the decrease of both the oxygen anions and phosphorous cations in the glass network [27], which increases the relative ratio of strontium to oxygen in the glass network. This in turn increases the connectivity of the oxygen network. Also, the gradual migration of iron from GNM to GNF positions may act to increase the hardness due to the formation of the strengthened Fe---O bond replacing the week P---O bond in the glass network.

Magnetic Susceptibility

The volume magnetic susceptibility as well as the calculated mass- and molar magnetic susceptibility values are exhibited in Table (2), where all values indicated that all samples appeared to be paramagnetic materials [28], which was confirmed by the obtained ME results. The variation of the molar magnetic susceptibility as a function of SrO content is shown in Fig. (8).The data indicate that, the molar susceptibility values increased gradually as SrO was gradually increased. This increase can be explained to be due to two factors,

1- The gradual transformation of the ferrous to ferric cations in the studied glass samples, which was clearly observed in the Mossbauer data presented in Table (1), since ferric cations have five parallel spin electrons, aligned with the applied field, and this act to enhance the magnetization [28].

2- The gradual migration of Fe cations from FeO_6 groups to FeO_4 groups, (which was also confirmed by both IR and Mossbauer results), where, FeO_4 have higher magnetic moment than FeO_6 groups [28].

So, the gradual increase of the susceptibility with increasing SrO contend can be attributed to the transformation of ferrous to ferric as well as from FeO_6 to FeO_4 groups, which may be due to the gradual decrease of phosphorous cations [12].

Table2. Volume, mass and molar magnetic susceptibilities of the studied glass samples:

Samples	Volume-magnetic susceptibility (emu) *10^{-6}	Mass-magnetic susceptibility (emu.cm^{-3}.gm) *10^{-6}	Molar-magnetic susceptibility (emu.cm^{-3}.mol^{-1})*10^{-4}
3 SrO mol. %	2.91372	1.053772	0.801582
6 SrO mol. %	3.01998	1.09349	0.839134
9 SrO mol. %	4.56469	1.677219	1.298539
12 SrO mol. %	5.52851	1.95471	1.526971
15 SrO mol. %	6.69589	2.212207	1.743784

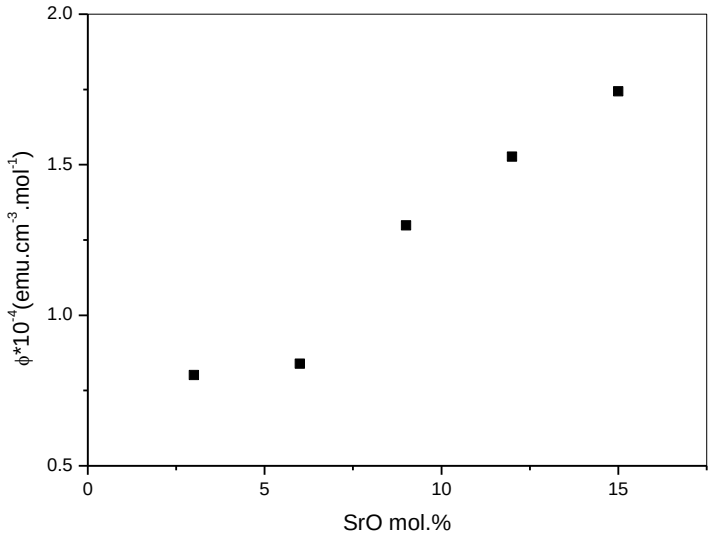

Fig.8: Molar magnetic susceptibility values as a function of SrO content.

Gamma-Ray Mass Attenuation Coefficient

The calculations of (μ/ρ) for various materials are useful and helpful for shielding design and construction. However, the shielding properties [(μ/ρ) and HVL] of the studied glasses will be checked now by calculating the gamma-ray mass attenuation coefficient (μ/ρ) using WIN X-COM program based on the mixture rule [17] at gamma-ray energies from 0.001 to 10 MeV [11]. The HVL values were then obtained applying equation (6), at low gamma-ray photon energies only [from 0.01 and 0.08 MeV]. The obtained values of (μ/ρ) as well as HVL at 0.2 MeV, are presented in Table (3) as SrO was gradually increased.

Table3. The obtained values of (μ/ρ) and HVL of the studied glasses as a function of SrO content at 0.2 MeV:

Sample no.	3 mol. % SrO	6 mol. % SrO	9 mol. % SrO	12 mol. % SrO	15 mol. % SrO
(μ/ρ) $cm^2.g^{-1}$	0.132	0.133	0.134	0.135	0.137
HVL cm	2.182	2.128	2.120	2.048	1.950

Fig. (9) Shows a log scale relation between the obtained values of (μ/ρ cm^2g^{-1}), as a function of gamma-ray photon energy in the range from 0.001 to 10 MeV (high and low gamma-ray energy). It appeared generally that the value of (μ/ρ) decreased gradually with the increase of photon energy. Also (μ/ρ) values show slight differences between the studied glasses, which can be attributed to the little differences in their measured densities. This figure shows also that the variation follows three different regions depend on the photon energy; region (I), from 0.001 to about 0.02 MeV and region (II) from 0.02 to about 0.2 MeV while region (III), from 0.2MeV to 10MeV.

In region (I), the (μ/ρ) shows sharp decrease with the increase of gamma-ray photon energy approximately for all glass samples. In this region, the predominant interaction is the absorbed photons by photoelectric effect [29].

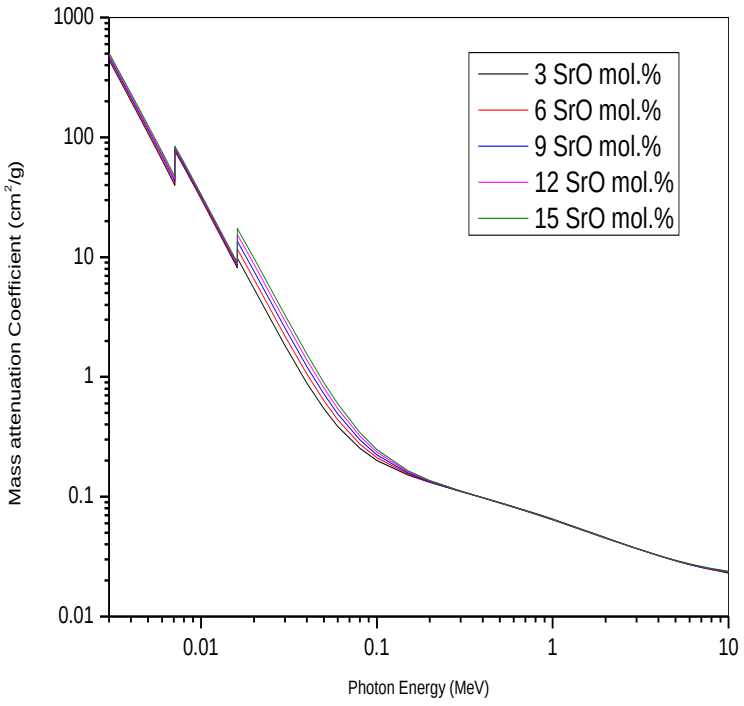

Fig.9: A log scale showing the change of (μ/ρ) with the applied gamma-ray photon energy from 0.001 and up to 10 MeV.

In region (II), (μ/ρ) shows also a gradual decrease with the increase of gamma-ray photon energy, approximately for all glasses, which can be attributed to the contribution of Compton scattering with photoelectric effect, but it can be also see that (μ/ρ) is proportional to SrO content. This behavior may be due to the fact that, Compton scattering is predominant at intermediate photon energies for atoms having intermediate Z atomic weight values, like (Sr) [Z=38 and A.W.= 87.62]. Therefore, both Compton scattering cross-section and photoelectric effect may be considered in this region.

In region (III), the values of (μ/ρ) show appreciable decrease also, with increasing photon energies for all glass samples [29, 30]. Fig. (10), exhibits the variation of (μ/ρ) as a function of only, low gamma-ray photon energies [between 0.01 and 0.08 MeV] for all the studied samples. However the observed increase in (μ/ρ) as well as the decrease of (HVL) can be attributed to the gradual increase of Sr^{+} cations. This in turn may be due to the fact that Sr^{+} cations act to fill the vacancies in the glass network and hence to decrease the internal free volume. Then the whole solid will have the ability to absorb low gamma-ray photon energies. That is, such solid glasses will act successfully as good gamma-ray attenuator especially at low photon energy. The sample containing 15 mol% SrO that exhibits the highest (μ/ρ) value and the lowest (HVL), can be considered the best shield among the studied samples and it can be used to capsulate the radio-active wastes before interment underground [31].

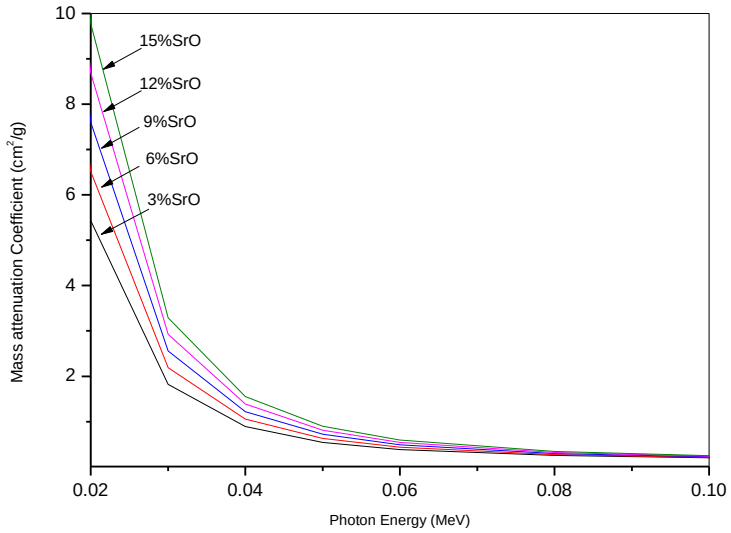

Fig.10: The variation of (μ/ρ) with the low gamma-ray photon energy (Compton scattering region).

CONCLUSION

According to the observations obtained during this study, the following conclusions can be drawn:

1- The gradual increase of SrO at the expense of P_2O_5 in the studied glasses acts in increasing the density and decreasing the molar volume, which may be due to the gradual decrease of the number of oxygen ion density of the glass network.

2- The increase of Sr^{+} and the decrease of P^{4+} gradually act to force iron cations to change from Fe^{2+} to Fe^{3+} state, and to migrate from GNM to occupy GNF positions, which was confirm by IR and ME analysis.

3- All samples exhibited paramagnetic character, and all magnetic susceptibility values increased gradually with increasing SrO content which was supposed to be due to the transformation of iron from Fe^{2+} to Fe^{3+} and from octahedral to tetrahedral coordination symmetry.

4- The micro-hardness increased gradually with increasing SrO content also, which may be due to increasing the ionic character of the network which increases the connectivity in the glass network.

5- The gamma-ray mass attenuation coefficient increased gradually with increasing Sr^{+} as a heavy metal cation. That is these glasses can be used as transparent shield, but at low gamma-ray photon energies only.

REFRENCES

[1] N. Chanthima, J. Kaewkhao & P. Limsuwan, J. Ann. Nucl. Energy, 41 (2012) 119.

[2] N. Chanthima, P. Prangsamrong, J. Kaewkhao & P. Limsuwan, J. Procidia Energy, 32 (2012) 976.

[3] A.G. Mostafa, H.A. Saudi, M.Y. Hassaan, S.M. Salem & S.S. Mohammed, American J. Modern Phys., 4 (4) (2015) 149.

[4] M. Kurudirek, Y. Ozdemir, O. Simsek & R. Durank, J. Nucl. Mater., 407 (2010) 110.

[5] A.A. Ramadan, A.G. Mostafa, M.Y. Hassaan, A.Z. Hussein, A.Y. Abdel-Haseib, Isotope & Rad. Res., 46 (1) (2014) 83.

[6] A. Al-Shahrani, A. Al-Hajry & M.M. El-Desoky, Phys. (B), Condens. Matter, 364 (1) (2005) 248.

[7] S.R. Manohara, S.M. Hanagodimath & L. Gerward, J. Nucl. Mater., 393 (2009) 465.

[8] H. Akamatsu, K. Fujita, S. Murai & K. Tanaka, Appl. Phys. Lett., 92 (25) (2008) 251908.

[9] A.G. Mostafa, M.Y. Hassaan, A.A. Ramadan, A.Z. Hussein & A.Y. Abdel-Haseib, Nature & Science, 11 (5) (2014) 148.

[10] S.N. Salama, H. Darwish & H.A. Abo-Mosallam, Ceram. International, 32 (2006) 357.

[11] N. Singh, R. Singh & K.J. Singh, Glass Technol., 46 (4) (2005) 311.

[12] F.A, Cotton & G.Wilkinson "Advanced Inorganic Chemistry" Wiley Eastern Private Limited (New Delhy) 2nd edition, 1980.

[13] H. Mori, H. Matsuno & H. Sakata, J. Non-Cryst. Solids, 267 (2000) 78.

[14] P. Zn_a_sik & M. Jamnick, J. Non-Cryst. Solids, 146 (1992) 74.

[15] C. Daynand & M.S. Graw, J. Mater. Sci., 31 (1966) 1945.

[16] P.P. Tasi & M. Greenblatt, J. Non-Cryst. Solids, 103 (1988) 101.

[17] A.M. Efimov, J. Non-Cryst. Solids, 209 (1997) 209.

[18] H.S. Liu, T.S. Chin & S.W. Yung, Phys. Chem. Glasses, 50 (1997) 1.

[19] M.C.R. Shastry & K. Rao, J. Spectrochim. Acta (A), 46 (1990) 1581.

[20] Y.M. Moustafa & K. El-Egili, J. Non-Cryst. Solids, 240 (1998) 144.

[21] L. Baia, D. Muresan, M. Baia, J. Popp. & S. Simon, Vib. Spectroscopy, 43 (2007) 313.

[22] D. A. Magdas, O. Cozar, V. Chis, I. Ardelean & N. Vedeanu, Vib. Spectrosc., 48 (2008) 25.

[23] G.K. Marasinghe, M. Karabulut, C.S. Ray, D.E. Day, M.G. Shumsky, W.B. Yelon, C.H. Booth, P.G. Allen & D.K. Shuh, J. Non-Cryst. Solids, 222 (1997) 144.

[24] X. Fang, C.S. Ray, A. Mogus-Milankovic & D.E. Day, J. Non-Cryst. Solids, 283(1-3) (2001) 162.

[25] A.M. Abdel-Ghany, A.A. Bendary,T.Z. Abou-El-Nasr, M.Y. Hassaan & A.G. Mostafa, Nature and Science, 12 (6) (2014) 139.

[26] M. Karabulut, E. Metwalli, D.E. Day & R.K. Brow, J. Non-Cryst. Solids, 328 (2003) 199.

[27] A.M. Abdel-Ghany, M.S.S.Saad, I.I. Bashter, T.Z. Amer, S.M. Salem & A.G. Mostafa, Nature and Science, 12 (12) (2014) 162.

[28] Ahmed Gamal El-Din Mostafa, Turk. J. Phys., 26 (2002) 441.

[29] L. Gerward, N. Guilbert, K.B. Jensen & H. Lerving, J. Radiat. Phys. Chem., 71 (2004) 653.

[30] I.I. Bashter, J. Ann. Nucl. Energy, 24 (1997) 1389.

[31] J. Kaewkhao, A. Pokaipisit & P. Limsuwan, J. Nucl. Mater., 399 (2010) 38.